INTERFACE

royalsocietypublishing.org/journal/rsif

Hot wings: thermal impacts of wing coloration on surface temperature during bird flight

Svana Rogalla[1], Liliana D'Alba[1], Ann Verdoodt[2] and Matthew D. Shawkey[1]

[1]Department of Biology, Evolution and Optics of Nanostructures Group, University of Ghent, K. L. Ledeganckstraat 35, 9000 Ghent, Belgium
[2]Department of Soil Management, Research Group Soil Degradation and Conservation, University of Ghent, Coupure Links 653, 9000 Ghent, Belgium

SR, 0000-0003-2972-7345; LD'A, 0000-0002-2478-3455; AV, 0000-0001-7995-9000; MDS, 0000-0002-5131-8209

Research

Check for updates

Cite this article: Rogalla S, D'Alba L, Verdoodt A, Shawkey MD. 2019 Hot wings: thermal impacts of wing coloration on surface temperature during bird flight. *J. R. Soc. Interface* **16**: 20190032.
http://dx.doi.org/10.1098/rsif.2019.0032

Received: 16 January 2019
Accepted: 1 July 2019

Subject Category:
Life Sciences–Physics interface

Subject Areas:
biomechanics, biophysics

Keywords:
colour, wing surface temperature, radiative heating, wind tunnel, bird flight, thermography

Author for correspondence:
Svana Rogalla
e-mail: srogalla@arcor.de

Electronic supplementary material is available online at https://dx.doi.org/10.6084/m9.figshare.c.4570217.

Recent studies on bird flight propose that hotter wing surfaces reduce skin friction drag, thereby improving flight efficiency (lift-to-drag ratio). Darker wings may in turn heat up faster under solar radiation than lighter wings. We used three methods to test the impact of colour on wing surface temperature. First, we modelled surface temperature based on reflectance measurements. Second, we used thermal imaging on live ospreys (*Pandion haliaetus*) to examine surface temperature changes with increasing solar irradiance. Third, we experimentally heated differently coloured wings in a wind tunnel and measured wing surface temperature at realistic flight speeds. Even under simulated flight conditions, darker wings consistently became hotter than pale wings. In white wings with black tips, the temperature differential produced convective currents towards the darker wing tips that could lead to an increase in lift. Additionally, a temperature differential between wing-spanning warm muscles and colder flight feathers could delay the flow separation above the wing, increasing flight efficiency. Together, these results suggest that wing coloration and muscle temperature both play important roles in modulating wing surface temperature and therefore potentially flight efficiency.

1. Introduction

Birds have tremendous diversity in plumage coloration produced by either selective absorption of light by pigments or coherent scattering of light by nanostructured materials (structural colours) [1]. Most studies on feather coloration focus on their potential functions in sexual or social signals [2] or in camouflage [3]. However, colours also have significant thermal properties [4]. In general, dark colours absorb more solar radiation than light colours, potentially leading to a faster increase in surface temperature [5]. Both plumage properties such as feather microstructure (e.g. density, number and placement of feathers on skin, fraction of feather surface), micro-optical properties (e.g. absorptivity, reflectivity, transmissivity) and coloration of plumage elements [6], as well as environmental factors such as incoming solar radiation (varying with season, latitude and time of day), ambient humidity and wind affect how the plumage surface warms. Even slight changes in wind speed can strongly affect solar heat gain, and more so of dark than light plumages [7]. Thus, it is critical to consider the effects of wind in conjunction with solar effects when studying the thermal properties of differently coloured feathers.

Overcoming drag and producing lift are the energetically costly mechanisms of flight [8]. Drag is directed opposite to the flight direction and is opposed by thrust, while lift is directed perpendicular to the flight direction and opposes the body weight imposed by gravity (electronic supplementary material, figure S1). Birds can use both active wing flapping to generate thrust or passive soaring to generate lift [8], with the former obviously more costly than the latter. Every improvement

THE ROYAL SOCIETY PUBLISHING

royalsocietypublishing.org/journal/rsif *J. R. Soc. Interface* **16**: 20190032

Figure 1. (*a*) Colour and (*b*) thermal images of live osprey wings (from left to right): open dorsal wing, open ventral wing and closed wings. AV1 refers to the coverts covering the muscular part of the wing; AV2 to the flight feathers. (Online version in colour.)

in flight efficiency, including adaptations in flight mode or wing shape, as well as coloration, may help reduce drag force and increase lift [9,10]. For instance, larger wings are known to create more lift [11], while a well-streamlined body reduces drag [12].

Darker wings could improve a bird's flight efficiency under highly intense solar radiation. The larger heat gain of a dark dorsal wing would lead to a decrease in air density on top of the wing, in turn reducing skin friction drag [10]. Likewise, a warmer ventral wing would reduce drag on the wing bottom but should heat less because it is not directly exposed to solar radiation [13]. However, only a couple of studies have addressed the impacts of wing coloration and surface temperature on birds' flight [10,13,14]. Through theoretical calculations of surface temperature for artificially painted black and white flat plates, the authors concluded that the temperature differences between brightly and darkly coloured top wings in albatrosses (Diomedeidae) resulted in differences of around 10°C [10] that under laminar conditions likely decreased skin friction drag force by up to 7.8% during flight [14]. Large birds flying between 6 and 18 m s^{-1} occupy an intermediate range of Reynolds numbers (which indicates whether fluid flow over a surface is steady or turbulent) between 15 000 and 500 000 [8]. For flat plates, this range indicates laminar conditions [15], while the flow regime of bird wings seems to be more complex and might lie in an intermediate [8] or even turbulent regime [16]. However, empirical tests of these results under realistic conditions are needed.

Here, we address the hypothesis that coloration can affect wing surface temperature. We used a combination of field and laboratory tests using osprey (*Pandion haliaetus*), northern gannet (*Morus bassanus*) and lesser black-backed gulls (*Larus fuscus*) as study species. All three species are migratory. Ospreys are cosmopolitan long-distance daytime [17] migrants moving between Europe and sub-Saharan Africa and southeast Asia [18] that have brown wings with a counter-shaded coloration pattern (dark dorsum and light ventral surface). Adult gannets have white wings on both sides with black wing tips, while juveniles have dark grey feathers. Lesser black-backed gulls have counter-shaded wings with light grey dorsal surfaces. We predicted that darker dorsal wings would become hotter than brighter wings and that these effects would be mitigated by wind speed. We further predicted that dorsal surface temperature is more strongly affected by solar radiation than the ventral surface temperature, suggesting that the colour of the dorsal wing plays a more predominant role in drag reduction than colour and temperature of the ventral wing.

2. Material and methods

We tested our hypothesis in three ways.

First, we used reflectance data to calculate the dorsal surface temperature of differently coloured wings at varying solar irradiance and wind speeds. We then used thermal imaging to measure wing surface temperature on live ospreys. Finally, we experimentally heated prepared wings of different colours in a wind tunnel to measure the impact of colour, radiation and wind on wing surface temperature.

2.1. Sample collection and preparation

We obtained feather samples from 11 live ospreys. To measure plumage reflectance, we collected three coverts at a homogeneously coloured part of both the dorsal and ventral wing (figure 1). We further obtained 10 wings from differently coloured species (electronic supplementary material, figure S2): four osprey wings (dark brown) and two wings each of an adult northern gannet (white wings with black tips), a juvenile northern gannet (dark grey) and a lesser black-backed gull (light grey). We measured reflectance within the UV–VIS–NIR range (300–2100 nm) using a dual spectrophotometer and light source (AvaLight-DH-S Deuterium-Halogen Light Source and AvaLight-HAL-(S)-MINITungsten-Halogen Light Source) set-up (Avantes Inc., Broomfield, CO, USA) (for further details, see electronic supplementary material). To prepare the wings for the wind tunnel experiment, we removed the muscles and flesh from the wings and opened them for drying. To simulate the internal heat produced by the bird on the ventral wing side according to temperatures measured in live birds, we inserted multiple ThermaCare heat pads (each with a dimension of 2 cm × 1 cm) in the humerus and forearm region of the dried wing and fixed them with Micropore tape beneath the skin. The heat pads have a constant temperature of 40°C for 8 h and are thus well suited to simulate temperature values and heat distribution on the ventral wing site of live birds (electronic supplementary material, figure S3).

2.2. Surface temperature modelling

We calculated the dorsal wing surface temperature based on reflectance measurements in live ospreys and in dried wings following the approach of Hassanalian *et al*. [10]. To model surface temperatures, we used the calculator from the LBNL Heat Island Group (LBNL-SRI) [19] for horizontal and low-sloped (less than 9.5°) opaque surfaces. We calculated the dorsal wing surface temperature as the steady-state surface temperature (T_S) for a surface exposed to the Sun with

$$\alpha \times I = \varepsilon \times \sigma \times (T_S^4 - T_{Sky}^4) + h_C \times (T_S - T_a),$$

where α is solar absorptance, I is solar irradiance, ε is the thermal emissivity, σ is the Stefan–Boltzmann constant ($5.670 \times 10^{-8}\ \mathrm{W\ m^{-2} \cdot K^{-4}}$), T_{Sky} is the sky temperature, h_C is the convective coefficient and T_a is the air temperature [20]. Solar absorptance is 1 minus the mean reflectance measured in wings and feathers (electronic supplementary material, table S1). For solar irradiance, we included values ranging from 0 to 1000 W m^{-2}. An intensity of 1000 W m^{-2} is comparable to the irradiance reaching the Earth's surface on a sunny day [21]. We set emissivity ε at 0.95, which is the standard value used for biological tissue [22]. We set air temperature as the average air temperatures measured for live ospreys (22°C) and as the average of each trial for the wind tunnel measurements (minimum temperature: 15.6°C, average temperature: 24.8°C, maximum temperature: 31.0°C). Under the open sky, thus for the temperature measurements on live birds, the sky temperature can be expressed as

$$T_{Sky} = \varepsilon_{Sky}^{0.25} \times T_a.$$

with ε_{Sky} as sky emissivity [23]. The emissivity of the sky can be defined with the dew point temperature T_{dp} as follows [23]:

$$\varepsilon_{Sky} = 0.742 + 0.0062 \times T_{dp}.$$

The dew point temperature can be expressed as

$$T_{dp} = 237.3 \times \frac{\ln \mathrm{RH} + (17.27 \times T_a/(T_a + 237.3))}{17.27 - \ln \mathrm{RH} - (17.27 \times T_a/(T_a + 237.3))} (^\circ\mathrm{C}),$$

where RH refers to the relative humidity, which was set as 0.7 (average humidity measured for live birds), thus T_{Sky} was 9.7°C for live ospreys. For the wind tunnel experiment, T_{Sky} was set corresponding to the temperature of the tunnel walls. As an approximation for the temperature of the tunnel walls, we set T_{Sky} as air temperature T_a. The convective coefficients are directly correlated to wind speed. We set wind speeds according to flight speeds (6, 12, 18 m s^{-1} (table 1)). The corresponding convective coefficients were 10.5, 32.9, 38.7, 41.8 W m$^{-2} \cdot$ K^{-1} [28]. This model for steady-state surface temperature (T_S) assumes that the conduction into the material is zero. For plumage (penguin feathers) conduction is only 1.93 W m$^{-1} \cdot$ K^{-1} [29].

2.3. Measurements on live birds

To assess the effect of incoming solar radiation on the surface temperature of live birds, we took thermograms of 11 juvenile ospreys housed at the Biosphere Reserve of Urdaibai (Biscay, Basque Country, Spain) as part of a reintroduction project from a Scottish population. Juvenile ospreys were brown and varied only slightly in brightness (electronic supplementary material, figure S4). The climate in the reserve is Atlantic, with mean annual temperatures of 14.5°C, and an average yearly precipitation of *ca* 1700 mm. Five to

Table 1. Morphometric data (Pennycuick [24], Shamoun-Baranes & van Loon [25]) and recorded flight speeds of ospreys, gannets and lesser black-backed gulls as mean values or ranges.

	wing span (m)	wing area (m^2)	body mass (kg)	wing Reynolds number	recorded flight speeds (m s^{-1}) gliding/soaring	flap-gliding	continuous flapping	source
osprey	1.59	0.3	1.49	154 800–253 700	10–14	5–20	11–18	[26]
(*Pandion haliaetus*)					5.2–10.2	6.5–13.5	–	[17]
northern gannet (*Morus bassanus*)	1.85	0.262	3.01	136 400–208 400		14.9		[27]
lesser black-backed gull (*Larus fuscus*)	1.43	0.243	0.77	118 300–196 800	15.5 ± 5.0		13.6 ± 3.5	[25]

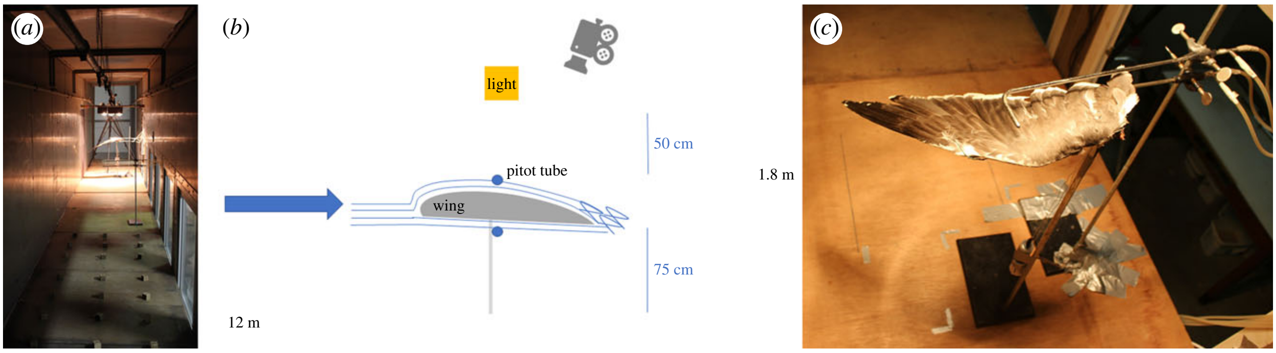

Figure 2. Set-up for the heating experiment on differently coloured wings in the wind tunnel: (*a*) frontal view, (*b*) side view (scheme) and (*c*) top view of wing. Wings were exposed to radiation intensities of 0, 500 and 1000 W m^{-2} and wind speeds of 6, 12 and 18 m s^{-1} to measure how feather coloration affects surface temperature during flight. Surface temperature was measured with a thermal camera installed above the wings. (Online version in colour.)

six weeks after the ospreys hatched (11 July 2017) they were transported to Urdaibai and kept in a hacking tower until fledging. At an age of seven to nine weeks, all ospreys were able to fly and in early September they started their migration to Senegal (confirmed by GPS data). We measured and weighed the birds immediately after their arrival and 2 days before being released (departure dates: 19, 25 July, 7 August). We measured plumage surface temperature using thermal imaging. We used a Testo 875 Thermal Imager (160 × 120 pixel array sensitive to 8–14 µm, accuracy ± 2°C/±2%) with the emissivity ε set at 0.95 [22]. Images were stored as .bmt files and processed with IRSoft (Testo SE & Co. KGaA, Lenzkirch, Germany).

We took thermograms under two different circumstances: first, with the bird in hand, and, second, with the birds freestanding in the hacking tower. While holding the bird we took four thermal images per individual at night and thus without any incoming solar radiation. Photos were taken with first closed and then open dorsal and ventral wings at 1.1 m distance. As a reference, we included a black-painted wooden plate ($\varepsilon = 0.95$) with an attached thermocouple (Tinytag Talk 2) in each picture. We measured temperature and humidity with a thermo-hygrometer (ETI Hygro-Thermo Pocket-Sized Hygrometer) and wind speed with an anemometer (HoldPeak HP-846A).

The ospreys were placed in four cabins (1.45 × 1.90 m) in the hacking tower (electronic supplementary material, figure S5). Those cabins were covered above, partially covered towards north and south and open at the west side. Thus, birds were partly exposed to wind and solar radiation. We took the thermograms through a hole 20 cm above the ground level of the hacking tower. Camera-to-bird distance ranged from 0.3 to 1.7 m and depended on where the ospreys moved within their cabin. At 1.1 m distance, we placed the same temperature reference as mentioned before. Apart from temperature, humidity and wind speed measurements, we further assessed the incoming solar irradiance in W m^{-2} with a pyranometer (Dr Meter® SM206 Digital Solar BTU Power Meter). For each thermogram we measured the irradiance beneath the hacking tower, pointing the pyranometer horizontally to the west, namely the open side of the hacking (electronic supplementary material, figure S5). We further recorded the wind speed for each thermogram at the same location (electronic supplementary material, figure S5).

A total of 2225 thermograms were taken at air temperatures ranging from 16.5°C to 32.3°C, irradiance of up to 870 W m^{-2} and maximum wind speeds of 2.9 m s^{-1}. Sample size varied for each individual (electronic supplementary material, table S2) and depended on how often the birds moved in front of the camera. In total, we obtained 4021 average temperature values for different body parts and positions (closed versus open, dorsal versus ventral wings, muscular wing part versus flight feathers (figure 1; electronic supplementary material, table S2). No pictures were taken at wind speeds exceeding 3 m s^{-1} coming from the open side of the tower [30] or high precipitation [31], to avoid the loss of accuracy in the temperature measurements.

2.4. Measurements on wings

To test the impact of mean brightness on wing surface temperature, we exposed 10 prepared wings (four osprey wings, four gannet wings (juvenile + adult) and two wings from a lesser black-backed gull; see electronic supplementary material, figure S2) to a radiation source of 1000 W m^{-2} for 10 min. Mean brightness was measured with spectrophotometry (see Sample collection and preparation). Wing surface temperature was assessed with an FLIR T530 Thermal Imager (FLIR Systems Inc., Oregon, USA). We took three repeated measurements per wing.

To simulate flight and measure the impact of wind on wing surface temperature, we performed the heating experiment in the wind tunnel at the International Centre for Eremology (I.C.E.), Ghent University, Ghent, Belgium. The wind tunnel is a closed-circuit low-speed blowing-type tunnel with an axial fan, 1.5 m in diameter. The dimensions of the test section are 12 m length and 1.2 m width, while the adjustable roof height was set at 1.8 m for the experiment. Boundary layer thickness was adjusted as well to ensure a constant wind velocity within 0.5–0.9 m height, and that the flow was parallel to the tunnel wall. Turbulence intensity is unknown since the instrumentation to measure wind-velocity fluctuations at a very high measuring frequency is not available at I.C.E. However, based on Gabriels *et al.* [32] the anemometers give reliable results. For flight simulation, each wing was attached to a pole at the end of the humerus and placed horizontally (angle of attack approx. 0°) in the wind tunnel 75 cm above the ground (figure 2). We measured the wind speed with pitot tubes (Testo 0638.1545, accuracy = ±10 Pa; Testo SE & Co. KGaA, Lenzkirch, Germany) at the entrance of the wind tunnel. Reynolds numbers of osprey, gannet and gull wings ranged from 118 300 to 253 700 at sea level (table 1). To simulate flight, we chose wind speeds of 6, 12 and 18 m s^{-1}, which are similar to flight speeds recorded in all our study species (table 1).

We heated the wing with five infrared light bulbs that produce radiation similar to that reaching the Earth's surface (Phillips IR 250 W; electronic supplementary material, figure S6), installed 50 cm above the wing. For each trial, we heated the wing for 2 min and then started the wind for another 2 min. Solar irradiance was set according to values that reach the Earth's surface (500 and 1000 W m^{-2}) [21]; see electronic supplementary material, figure S7). As a reference, we measured wing surface temperature without radiation at all wind speeds. Trials were performed three times per wing. Once exposed to wind, wing surface temperature would quickly decline and stabilize (electronic supplementary material, figure S8). For statistical analyses, we averaged the stabilized values (all values for irradiance = 0 W m^{-2}; greater than 140 s for irradiance greater than 0 W m^{-2}).

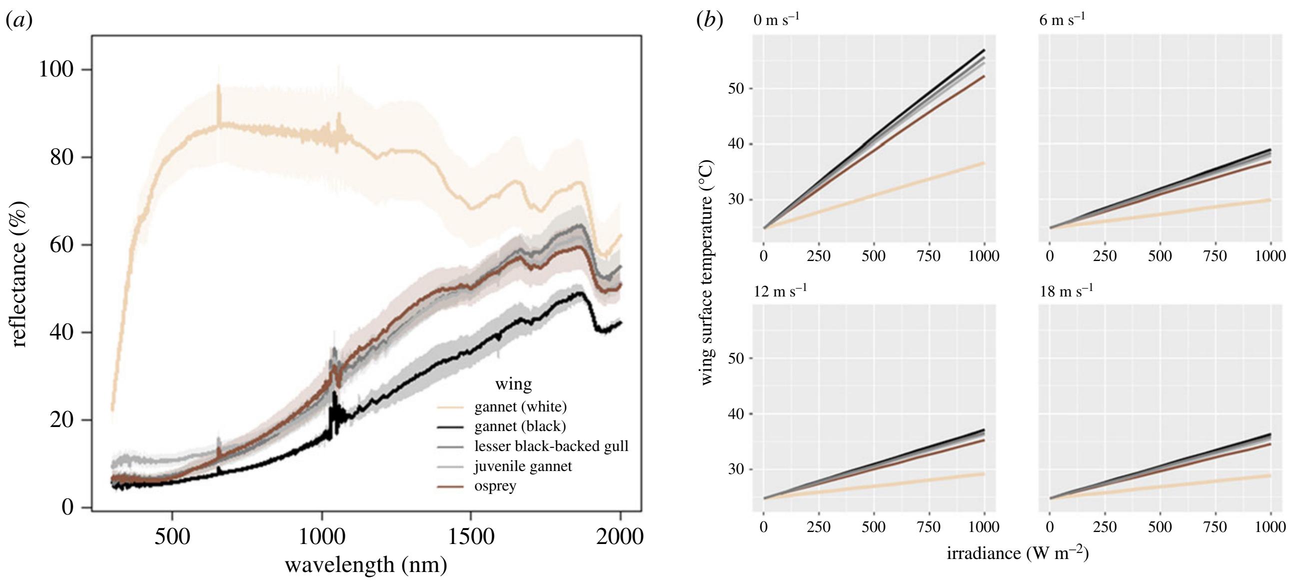

Figure 3. (*a*) Spectral reflectance curve of differently coloured wings used in the wind tunnel experiment and (*b*) modelled surface temperature as a function of increasing solar irradiance and at varying wind speeds. Lighter wings reflect more light (*a*) and are predicted to heat less at all wind speeds than darker wings (*b*). (Online version in colour.)

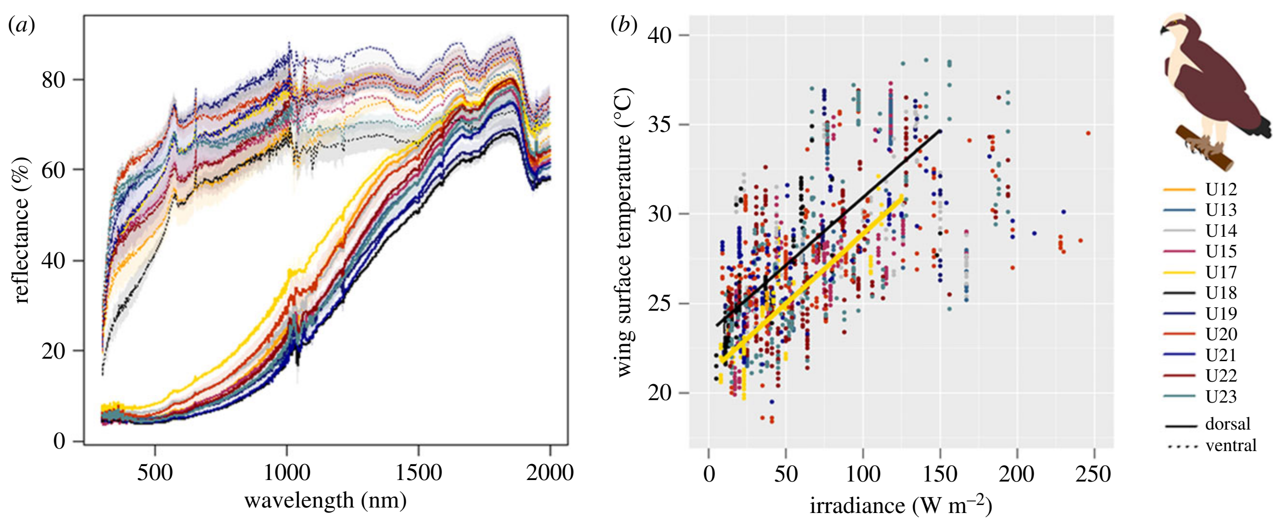

Figure 4. (*a*) Spectral reflectance curve of osprey feathers (dorsal and ventral wing coverts) per individual (named by ring number: U12–U23). (*b*) Increase in dorsal wing surface temperature with solar irradiance measured in live birds in the absence of wind. Linear correlations between radiation and wing surface temperature are shown for the brightest (U17) and darkest (U18) individual for the muscular part of closed wings. Brighter feathers heat less than darker feathers. (Online version in colour.)

Dorsal wing surface temperature was assessed with a High Sensitivity MWIR Performance Camera (FLIR X6520sc; FLIR Systems Inc., Oregon, USA) installed 80 cm above the wing (figure 2). The camera produces 640 × 512 full-frame imagery at speeds up to 146 Hz, with integration times as short as 80 ns for accurate measurement of high-speed processes, such as during the application of wind. Thermal videos were analysed with ResearchIR (FLIR Systems Inc.). We measured the surface temperature of ventral flight feathers with a thermocouple (Tinytag Talk 2) attached to the ventral wing and covered by one feather. We assessed the ventral surface temperature of the imitated muscles with thermal imaging on an osprey wing placed upside down in the wind tunnel three times per wind speed ($n = 9$).

To explore how a black-and-white gannet wing heats up in comparison with a unicoloured wing, we visualized air movements above the heated wings in the thermal videos. To do so, we applied the filter 'sliding subtraction' in Research IR. This filter subtracts the previous frames from the current frame and thus visualizes heat differentials and air movements. To examine whether a separation of the boundary layer above the wing takes place [12], we visualized the wind flow with fine powder for all wings.

2.5. Statistical analysis

To explore the relationship between wing surface temperature, wing coloration and environmental variables in live birds, we used an all-subsets approach to fit a set of linear models with wing surface temperature as a response variable. We first examined possible predictor variables for evidence of multi-collinearity and found that several variables were highly correlated (electronic supplementary material, table S3). Therefore, in building the sets of candidate models, we avoided using correlated terms in the same models. In total, we evaluated 47 models (see electronic supplementary material, table S4 for a full list of candidate models) with different combinations of the following predictor variables: radiation, air temperature, wind speed, camera distance, departure

Table 2. Top three general linear models for osprey wing surface temperature measured in live birds (n = sample size). Bold indicates the best model in each category.

model	K	rank	ΔAICc	weight
closed dorsal wing (muscular) ($n = 1795$)				
radiation + air temperature × wind speed + camera distance + mean brightness	9	**1**	0	**0.94**
radiation + air temperature × wind speed + camera distance	8	2	6.76	0.03
radiation × air temperature × wind speed + camera distance + mean brightness	12	3	7.60	0.02
closed dorsal wing (flight feathers) ($n = 1458$)				
radiation + air temperature + wind speed + camera distance + mean brightness	8	**1**	0	**0.82**
radiation + air temperature × wind speed + camera distance + mean brightness	9	2	4.81	0.07
radiation + air temperature + wind speed + camera distance	7	3	5.76	0.04
open dorsal wing (muscular) ($n = 263$)				
radiation + air temperature + wind speed + camera distance + mean brightness	8	**1**	0	**0.82**
radiation + air temperature + wind speed + camera distance	7	2	4.29	0.10
radiation + air temperature × wind speed + camera distance + mean brightness	9	3	5.06	0.07
open dorsal wing (flight feathers) ($n = 257$)				
radiation + air temperature + wind speed + camera distance + mean brightness	8	**1**	0	**0.52**
radiation + air temperature × wind speed + camera distance + mean brightness	9	2	1.37	0.26
radiation + air temperature + wind speed + camera distance	7	3	3.41	0.09
open ventral wing (muscular) ($n = 141$)				
air temperature + mean brightness	5	**1**	0	**0.79**
air temperature	4	2	4.05	0.11
radiation + air temperature + wind speed + camera distance + mean brightness	8	3	4.95	0.07
open ventral wing (flight feathers) ($n = 107$)				
air temperature + mean brightness	5	**1**	0	**0.77**
air temperature	4	2	2.52	0.22
radiation + air temperature + mean brightness	6	3	9.55	0.01

weight and mean brightness. We ranked the models based on Akaike's information criterion corrected for small sample size (AICc) [33]. We calculated the evidence ratio [33] as a measure of relative fit of models that included both environmental variables and wing coloration versus those that included only environmental variables. We obtained the estimates and 95% confidence intervals of each variable included in the best model to evaluate which of the variables has a significant effect on surface temperature. We found an effect of camera distance on temperature measurements in live ospreys that can be explained with the atmosphere's self-radiation [34]. However, temperature differences are marginal and can be neglected (see electronic supplementary material). To compare dorsal with ventral wing surface temperature and reference with thermal camera measurements, we applied a paired t-test.

For dried wings, we tested the impact of mean brightness on maximum wing surface temperature for the 10 min heating curves in a generalized linear model (GLM). To explore the impact of wind on wing surface temperature, we used an all-subsets approach as described above and included the following variables: feather absorbance, radiation, air temperature and wind speed. In total, we evaluated 24 models (electronic supplementary material, table S4). We compared dorsal with ventral wing surface temperature in a paired t-test. We further applied paired t-tests to compare surface temperature measurements of live birds and dried wings with the values predicted from our model. For all experiments using different thermal cameras, we calculated the repeatability according to Lessells & Boag [35] (see electronic supplementary material). We ran all our statistical analysis in R [36] using the following packages: dplyr [37], lme4 [38] and pavo [39]. For data visualization, we used ggplot2 [40].

3. Results

3.1. Surface temperature modelling

As predicted, our models estimated greater heating effects for darker, less reflective wings than for brighter dorsal wings with increasing solar radiation (figure 3); however, the differences in surface temperature seem to be most predominant between white (gannet) wings and the darker wings of the other species. In addition, wing surface temperature increases with solar radiation and is strongly affected by wind, while the effect of speed itself seems to be marginal (figure 3).

3.2. Measurements on live birds

Surface temperature differed between wing parts in live ospreys. For instance, coverts above the muscular part of the wing were 2.3°C warmer than flight feathers ($t = 36.38$, $p < 0.001$). However, we found strong evidence that dorsal wing surface temperature is affected by wing coloration (figure 4) and wind. For all dorsal wing parts and positions in live ospreys, the surface temperature increased with solar radiation and air temperature and decreased with wind, camera distance and dorsal mean brightness (tables 2 and 3). With ΔAICc

Table 3. Estimates of predictor variables in candidate models to explain osprey wing surface temperature.

	estimate	s.d.	*t*-value	95% CI
closed dorsal wing (muscular)				
intercept	5.54	2.65	2.09	0.71, 10.37
radiation	0.01	0.00	20.02	0.01, 0.01
air temperature	1.05	0.01	79.30	1.02, 1.08
wind	−0.23	0.07	−3.24	−0.36, −0.09
camera distance	−0.49	0.13	−3.88	−0.74, −0.25
mean brightness	−8.16	4.38	−1.87	−16.15, −0.19
departure weight	0.00	0.00	1.02	−0.00, 0.00
closed dorsal wing (flight feathers)				
intercept	2.89	1.77	1.63	−0.52, 6.33
radiation	0.01	0.00	17.06	0.01, 0.01
air temperature	1.13	0.01	88.75	1.10, 1.15
wind	0.04	0.07	0.52	−0.10, 0.18
camera distance	−0.28	0.12	−2.39	−0.50, −0.05
mean brightness	−8.18	4.75	−1.72	−17.44, 0.96
open dorsal wing (muscular)				
intercept	7.76	3.04	2.56	2.01, 13.61
radiation	0.01	0.00	9.64	0.01, 0.01
air temperature	0.94	0.05	20.25	0.85, 1.03
wind	−0.41	0.18	−2.25	−0.77, −0.06
camera distance	−2.07	0.44	−4.67	−2.95, −1.23
mean brightness	5.51	7.59	0.73	−9.29, 19.94
open dorsal wing (flight feathers)				
intercept	5.17	2.07	2.50	1.23, 9.18
radiation	0.01	0.00	5.14	0.01, 0.01
air temperature	1.03	0.04	26.24	0.96, 1.11
wind	−0.08	0.15	−0.56	−0.37, 0.20
camera distance	−1.02	0.35	−2.89	−1.70, −0.34
mean brightness	−3.66	4.96	−0.74	−13.38, 5.76
open ventral wing (muscular)				
intercept	17.65	3.23	5.47	11.43, 23.80
air temperature	0.76	0.06	13.36	0.65, 0.88
mean brightness	−5.26	4.41	−1.19	−13.67, 3.34
open ventral wing (flight feathers)				
intercept	4.36	2.19	1.99	0.09, 8.63
air temperature	1.09	0.05	24.28	1.00, 1.18
mean brightness	−2.53	2.84	−0.89	−8.07, 3.00

greater than 2 [33], there was much less support for any other model to explain dorsal wing surface temperature. Ventral wing surface temperature of live ospreys increased with air temperature and decreased with mean brightness of the ventral side (tables 2 and 3).

Dorsal feather surfaces in live ospreys were significantly ($p < 0.001$) warmer than predicted for all body parts and wing positions (table 4 and figure 5). While surface temperatures of flight feathers exceeded the predicted values by 4.9°C, the muscular part was about 7.3°C warmer than expected (table 4).

Dorsal wing surface temperatures of live ospreys differed significantly from ventral wing surface temperatures for muscles ($t = -6.98$, $p < 0.001$), but not for flight feathers ($t = -1.78$, $p = 0.095$). Under low radiation intensities, ventral wings were up to 3.5°C warmer than dorsal wings (electronic supplementary material, figure S9). Only for irradiance above 629 W m^{-2} did the muscular part of dorsal wings heat up more than the ventral wing parts (corresponding surface temperature = 40.3°C). For flight feathers though, the irradiance threshold was 175 W m^{-2} (corresponding surface temperature = 28.7°C).

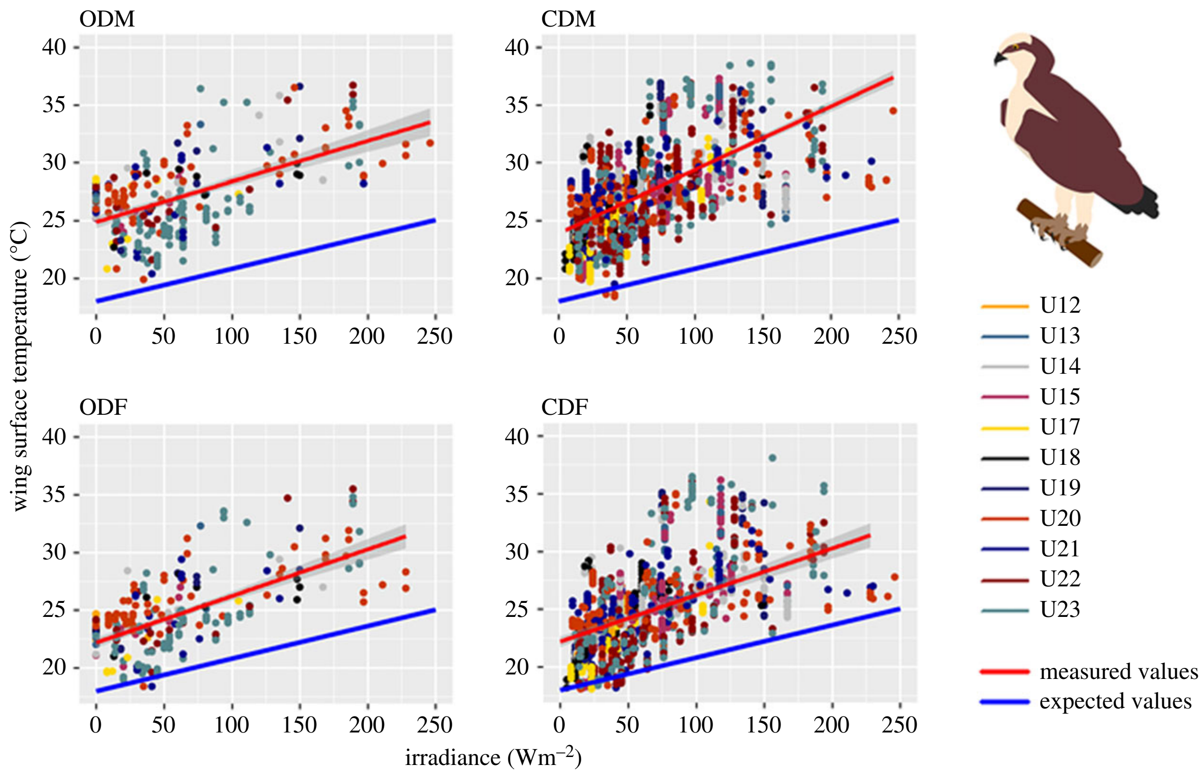

Figure 5. Increase in dorsal wing surface temperature with solar irradiance measured in live birds in different body parts and wing positions: muscular part of open dorsal wing (ODM), flight feathers of open dorsal wing (ODF), muscular part of closed dorsal wing (CDM) and flight feathers of closed dorsal wing (CDF). Different coloured dots represent individuals (labelled by ring number: U12–U23), while the lines represent the measured versus the expected values according to our models of surface temperature. (Online version in colour.)

Table 4. Comparison between measured and predicted wing surface temperatures in live ospreys in relation to solar irradiance ($y = 0.028x + 18$ for an average air temperature of 22°C) for all body parts and positions: ODM = open dorsal wing (muscular part), ODF = open dorsal wing (flight feathers), CDM = closed dorsal wing (muscular part), CDF = closed dorsal wing (flight feathers). Average air temperature was 22.1 ± 0.07°C.

	regression	*t*-value	d.f.	*p*-value	mean difference
ODM	$y = 0.024\,x + 25.550$	39.31	262	<0.001	7.2
ODF	$y = 0.035\,x + 22.476$	29.69	256	<0.001	4.9
CDM	$y = 0.021\,x + 26.000$	85.54	1794	<0.001	7.4
CDF	$y = 0.022\,x + 23.380$	50.89	1457	<0.001	4.9

Reference temperatures assessed with the Testo 875 Thermal Imager were 1.6°C warmer than the measurements with thermocouples ($t = 75.64$, $p < 0.001$). However, the mean of the differences lies within the error range of the thermal camera (accuracy: ±2°C).

3.3. Measurements on wings

When we included the imitation muscles in the dried bird wings, we found temperature differentials between dorsal muscles and flight feathers similar to those in live birds. At all wind speeds and in the absence of radiation, coverts above the muscular part of the wing were 0.2°C warmer than flight feathers ($t = 8.78$, $p < 0.001$); at 500 W m^{-2} they were 1.3°C warmer ($t = 9.65$, $p < 0.001$) and at 1000 W m^{-2} they were 2.0°C warmer ($t = 10.27$, $p < 0.001$).

In the absence of wind, darker feathers warmed significantly more than brighter ones when exposed to radiation (figure 6). With a maximum temperature of 70.7°C black feathers became up to 31.0°C hotter than white feathers (figure 6). We found a significant negative correlation between maximum wing surface temperature and mean brightness for both flight feathers ($r = 0.91$, $p < 0.001$) and imitation muscles ($r = 0.72$, $p = 0.005$) of dried wings. Even in the presence of wind, darker wings were warmer than brighter wings (figure 7). With a maximum temperature of 38.8°C black feathers became up to 8.9°C hotter than white feathers at wind speeds of 6 m s^{-1} (figure 7). Dorsal wing surface temperature decreased with wind speed but increased with radiation, air temperature and the interaction of radiation and absorbance (tables 5 and 6). Absorbance alone did not affect surface temperature (table 6). Ventral surface temperature above the imitation muscles was best explained by air temperature alone, while ventral flight feathers were warmer at higher air temperature and radiation (tables 5 and 6).

Dorsal surface temperature of flight feathers ($t = -3.2$, $p < 0.01$) was lower than predicted, but the mean temperature difference between measurements and predictions was only

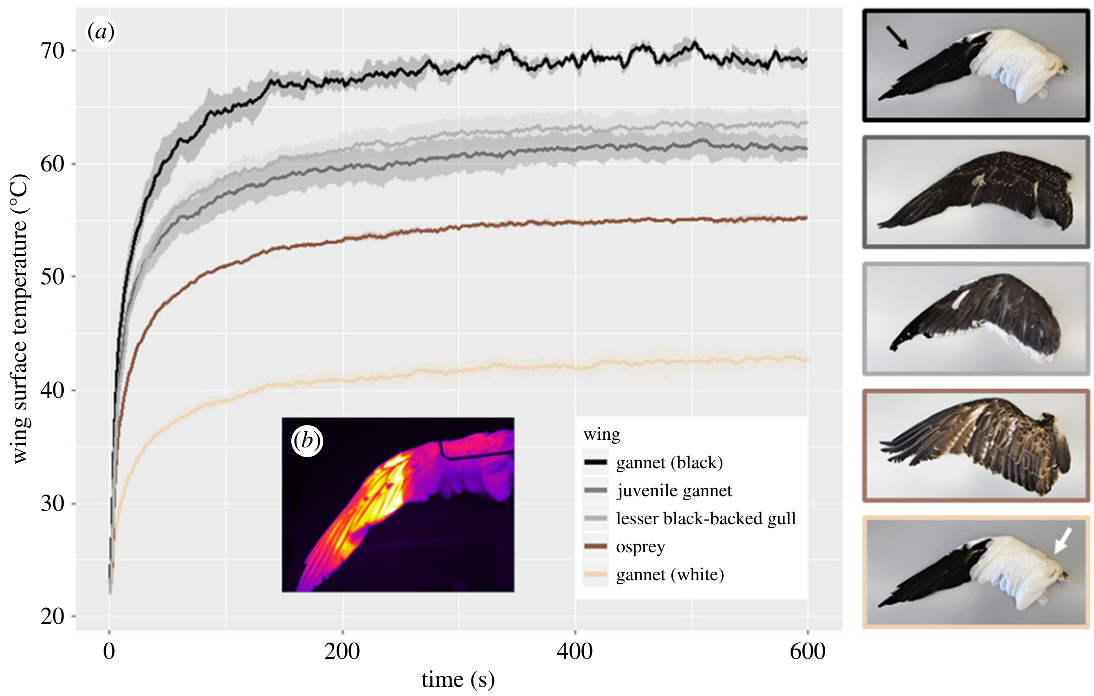

Figure 6. (*a*) Wing surface temperature of flight feathers during a 10 min heating process without wind. Heating curves are shown for the differently coloured wings exposed to an irradiance of 1000 W m^{-2} (graphic of left wings only). We show the mean values of three trials per wing and the standard deviation as the shaded area. (*b*) Thermal image of an adult gannet wing with brighter (yellow) colours representing hotter regions and darker (purple) colours denoting colder areas. (Online version in colour.)

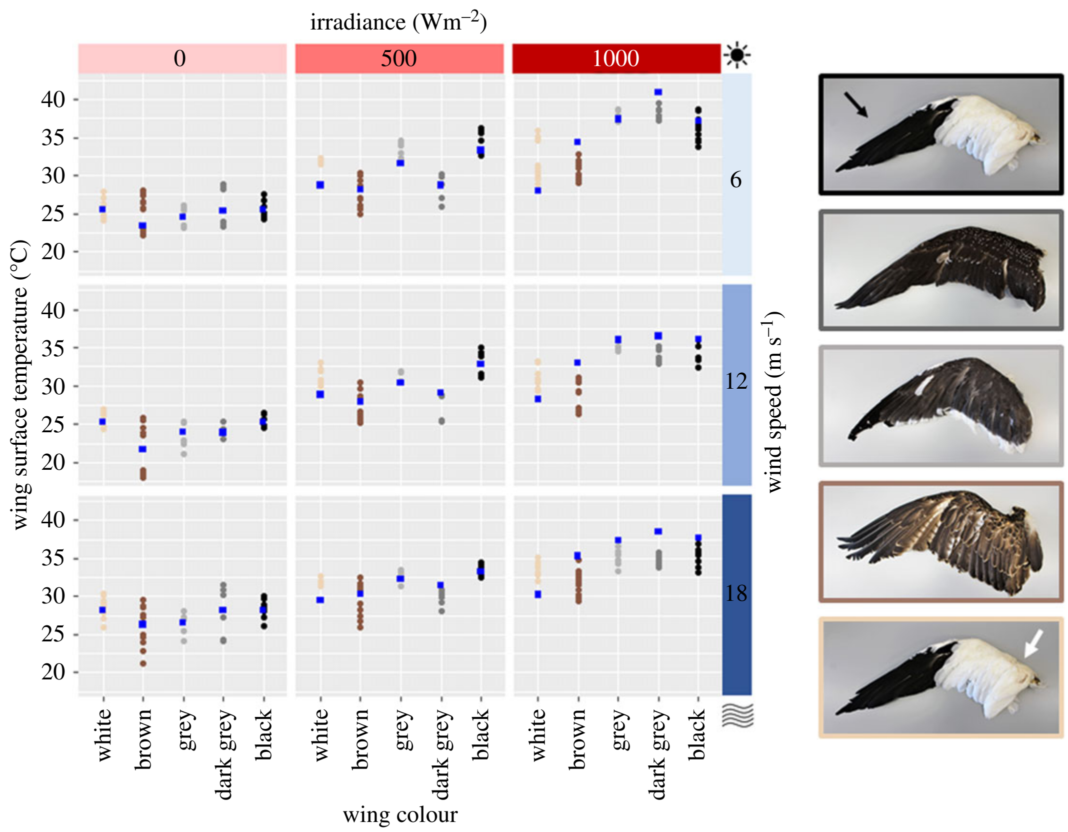

Figure 7. Mean wing surface temperature of differently coloured dorsal wings (flight feathers) at an irradiance of 0, 500 and 1000 W m^{-2} and at wind speeds of 6, 12 and 18 m s^{-1}. Average air temperature for the wind tunnel experiments was 24.8 ± 2.5°C. Blue squares show the predicted (modelled) mean temperatures. (Online version in colour.)

0.3°C, which lies within the error limits. However, the model to estimate surface temperatures tended to underestimate the heating of white (gannet) feathers, while it would overestimate the temperatures of darker feathers (figure 7). Surface temperature above the muscles was 1.1°C hotter than predicted ($t = 6.5$, $p < 0.001$).

Dorsal surfaces of dried wings were significantly warmer than ventral wings at an irradiance of 500 and 1000 W m^{-2} for

Table 5. Top three general linear models to explain wing surface temperature in dorsal and ventral wings measured in the wind tunnel (n = sample size). Bold indicates the best model in each category.

model	K	rank	ΔAICc	weight
dorsal wing (muscular) ($n = 368$)				
air temperature + wind speed + radiation × absorbance	8	**1**	0.00	**0.98**
air temperature × wind speed + radiation × absorbance	9	2	7.94	0.02
air temperature + wind speed + radiation + absorbance	7	3	27.99	0.00
dorsal wing (flight feathers) ($n = 368$)				
air temperature + wind speed + radiation × absorbance	8	**1**	0.00	**0.99**
air temperature × wind speed + radiation × absorbance	9	2	9.13	0.01
air temperature + wind speed + radiation + absorbance	7	3	14.69	0.00
ventral wing (muscular) ($n = 9$)				
air temperature	4	**1**	0.00	**1.00**
air temperature + wind speed	5	2	13.40	0.00
wind speed	4	3	15.02	0.00
ventral wing (flight feathers) ($n = 368$)				
air temperature + radiation	5	**1**	0.00	**0.86**
air temperature × wind speed + radiation	7	2	4.40	0.10
air temperature + wind speed + radiation	6	3	6.13	0.04

Table 6. Estimates of predictor variables in candidate models to explain wing surface temperature in the wind tunnel.

	estimate	s.d.	t-value	95% CI
dorsal wing (muscular)				
intercept	5.11	2.25	2.27	0.82, 9.41
air temperature	0.99	0.05	18.24	0.88, 1.10
wind speed	−0.31	0.03	−11.75	−0.36, −0.26
radiation	0.01	0.00	5.16	0.00, 0.01
absorbance	−0.77	3.86	−0.20	−8.23, 6.69
radiation × absorbance	0.01	0.00	6.56	0.01, 0.02
dorsal wing (flight feathers)				
intercept	3.90	1.70	2.29	0.65, 7.15
air temperature	0.97	0.04	23.14	0.89, 1.05
wind speed	−0.19	0.02	−9.16	−0.23, −0.15
radiation	0.01	0.00	6.93	0.00, 0.01
absorbance	−0.81	2.88	−0.28	−6.37, 4.73
radiation × absorbance	0.01	0.00	5.39	0.01, 0.01
ventral wing (muscular)				
intercept	4.00	4.04	0.99	−3.81, 11.80
air temperature	0.94	0.16	5.79	0.62, 1.25
ventral wing (flight feathers)				
intercept	2.28	0.59	3.85	1.12, 3.44
air temperature	0.93	0.02	41.25	0.89, 0.97
radiation	0.00	0.00	19.74	0.00, 0.00

all wind speeds (table 7; electronic supplementary material, figure S10). In the absence of radiation, ventral muscles were warmer than dorsal muscles, while temperature differences in dorsal and ventral flight feathers were marginal (table 7).

The significant temperature differential between black and white feathers in the gannet wing resulted in an increased airflow above the wing with convective currents flowing span-wise (i.e. from wing-root to wingtip) from brighter to darker

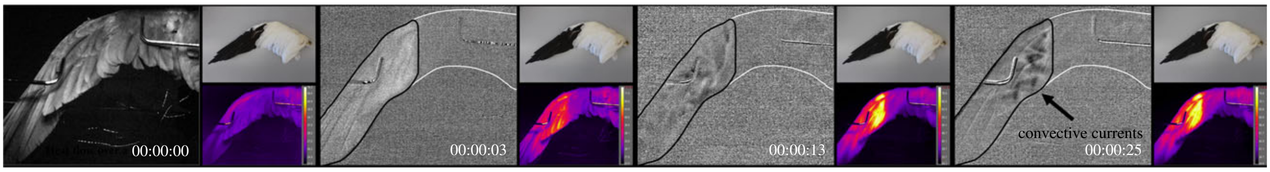

Figure 8. Air movement above gannet wing made visible with the filter 'sliding subtraction' (see electronic supplementary material, video). (Online version in colour.)

Table 7. Comparison between dorsal (DT) and ventral (VT) wing surface temperature for both muscles and flight feathers. Dorsal surface temperatures were assessed with thermography, ventral muscle temperature with thermography on a wing turned upside down in the wind tunnel and ventral flight feather temperature with a thermocouple attached to the feathers. Values shown are means (s.e.) measured at different wind speeds (m s^{-1}) and irradiance (W m^{-2}). For warmer dorsal than ventral wings, values are shaded in red; for warmer ventral than dorsal wings, values are shaded in blue (minimum difference 0.5°C). (Online version in colour.)

		irradiance		
		0	500	1000
muscles				
wind speed	6	DT = 25.2 (0.5) VT = 27.6 (0.6) $t = -4.74$ $p < 0.001$	DT = 32.9 (0.5) VT = 27.6 (0.6) $t = 11.58$ $p < 0.001$	DT = 36.9 (0.7) VT = 27.6 (0.6) $t = 12.86$ $p < 0.001$
	12	DT = 23.5 (0.5) VT = 26.2 (0.0) $t = -5.64$ $p < 0.001$	DT = 30.7 (0.4) VT = 26.2 (0.0) $t = 10.21$ $p < 0.001$	DT = 33.9 (0.5) VT = 26.2 (0.0) $t = 14.23$ $p < 0.001$
	18	DT = 27.6 (0. 4) VT = 28.2 (0.5) $t = -1.80$ $p = 0.079$	DT = 31.7 (0.3) VT = 28.2 (0.5) $t = 10.09$ $p < 0.001$	DT = 34.6 (0.4) VT = 28.2 (0.5) $t = 17.97$ $p < 0.001$
flight feathers				
wind speed	6	DT = 24.8 (0.5) VT = 24.8 (0.5) $t = 0.24$ $p = 0.816$	DT = 30.9 (0.5) VT = 25.8 (0.4) $t = 14.67$ $p < 0.001$	DT = 34.1 (0.5) VT = 27.0 (0.4) $t = 12.94$ $p < 0.001$
	12	DT = 23.3 (0.5) VT = 23.6 (0.5) $t = -3.63$ $p < 0.001$	DT = 29.4 (0.5) VT = 25.8 (0.4) $t = 9.97$ $p < 0.001$	DT = 32.0 (0.4) VT = 26.1 (0.3) $t = 10.63$ $p < 0.001$
	18	DT = 27.5 (0.4) VT = 28.2 (0.3) $t = -4.48$ $p < 0.001$	DT = 31.2 (0.4) VT = 28.2 (0.3) $t = 7.88$ $p < 0.001$	DT = 33.6 (0.3) VT = 28.9 (0.2) $t = 13.59$ $p < 0.001$

feathers (figure 8). As visualized with the thermal camera, this increased airflow indicates a higher mass flux above the wing. We found indications, such as feather fluttering, that boundary layer separation occurs above the dried wings (figure 9).

4. Discussion

We have clearly demonstrated, for the first time of which we are aware, that colours affect heating of bird wings under realistic flight conditions. We identified three main factors that affect wing surface temperature in a flying bird: most prominently, heating of darker dorsal wings under solar radiation, followed by the warmth of the ventral wing and of muscles and flight feathers.

4.1. Heating of darker dorsal wings

Darker dorsal wings were significantly warmer than brighter wings when exposed to solar radiation. This effect is

Figure 9. Visualization of the wind flow over an osprey wing (see electronic supplementary material, slow motion video). (Online version in colour.)

diminished, but not eliminated, by wind. Measured surface temperatures of flight feathers of dried wings were only marginally lower than predicted from our models, which shows that the model accurately estimates wing surface temperature during bird flight. Yet, the model tended to underestimate the heating of bright feathers, while it would overestimate the temperatures of dark feathers, indicating that wind has a stronger effect on dark than light plumages [7]. Interestingly, we found the effect of speed to be marginal, indicating that, once convection applies, the temperature differential in flight remains constant for all flight speeds. Darker wings heat up more than brighter wings when exposed to the same intensity of solar irradiance, even during flight. In the absence of solar radiation, however, colour does not affect wing surface temperature. The higher wing surface temperature of darker dorsal wings under high solar radiation could lead to a larger reduction in skin friction drag [10].

Temperature differentials were apparent even in the same side of the same wing, as demonstrated in the white gannet wing with black tips. Many birds, such as storks, cranes, pelicans and many gull species, are known for their mostly bright wing coverts and dark wing tips. The dark, highly melanized wing tips may protect the feathers from abrasion [41]. Apart from feather protection, we suggest that the temperature differential of a contrasting wing colour could also lead to greater spanwise mass flux above the wing, leading to an increase in dynamic pressure and thus to an increase in lift. Our dried wings with an angle of attack of 0° were not likely to produce any lift [42]. Future research will investigate the changes in flow patterns as a function of heating while the wings are at positive angles of attack relative to incurrent air.

4.2. Warmth of the ventral wing

In the absence of solar radiation, ventral osprey wings were warmer than dorsal wings. This pattern may be reinforced by ospreys' habit of mostly sitting with closed wings in the hacking tower. However, we found similar results for simulated muscle temperatures in dried wings used in the wind tunnel. Less-insulating feathers on the ventral site lead to higher surface temperatures that persist even during flight and may prevent overheating of the bird [43]. However, any increase in wing surface temperature on both the dorsal and ventral side could lead to a reduction in skin friction drag [13]. Therefore, not only ventral wing muscles but also the differential heating of ventral flight feathers with increasing solar radiation (indicating a rapid heat transfer through the feathers by conduction and convection [6]) could contribute to drag reduction during flight.

4.3. Warmth of muscles and flight feathers

Measurements in live birds were substantially larger than predicted, probably because of the absence of metabolic heat in the model. Surface temperatures above the muscular part were higher than those of flight feathers in both the dorsal and ventral wings of live birds. Even under high wind speeds, the imitation muscles (which maintained realistic temperatures) remained warmer than flight feathers and temperatures above the muscles were larger than predicted, indicating that the effect of body temperature on wing surface temperature is maintained during flight. This temperature gradient within the wing could influence the boundary layer. Heating the leading edge of an aerofoil delays transition, which means that flow separation occurs later above the wing, making flight more efficient by improving the lift-to-drag ratio [44,45]. We predict that the temperature differential between muscles and flight feathers could lead to the same effect. However, we still found evidence of boundary layer separation, such as feather fluttering, above the wing. This flow separation seems to occur in all wind tunnel measurements on prepared birds or parts of those for reasons not yet understood [46], but will be addressed in the future.

5. Conclusion

We found that wing surface temperature is affected by both muscle temperature and feather reflectance under exposure to solar radiation. While muscle temperature leads to a temperature gradient within the dorsal wing and increases the surface temperature of the ventral side, the heating of a darker dorsal wing exposed to solar radiation has a much stronger effect on wing surface temperature and could thus play a predominant role in drag reduction during flight. Future studies should directly explore to what extent wing coloration affects lift and drag when exposed to solar radiation.

Ethics. Thermal imaging on live ospreys was conducted as part of the following project: Galarza A, Zuberogoitia I. 2012 Osprey restoration project in the Urdaibai Biosphere Reserve (Basque Country). Urdaibai Bird Center/County Council of Biscay, Bilbao, Spain.

Data accessibility. Datasets for all experiments reported in this paper are publicly accessible in the Dryad data repository at https://doi.org/10.5061/dryad.hh23pt5 [47].

Authors' contributions. S.R. conceived the study, collected field data, designed and ran the experiments, analysed the data and drafted the manuscript. L.D'A. conceived the study, participated in the data analysis and critically revised the manuscript. A.V. participated in the design of the experiments and assisted with data collection. M.D.S. conceived and coordinated the study and critically revised the manuscript. All authors gave final approval for publication and agree to be held accountable for the work performed therein.

Competing interests. We declare we have no competing interests.

Funding. This work was supported by the Research Foundation—Flanders (FWO) (GOG2217N) and the US Air Force Office of Scientific Research (FA9550-18-1-0477).

Acknowledgements. We are deeply thankful for the great support from the Urdaibai Bird Center with sample collection on live ospreys, which includes the supply of feather samples and wings. Particularly we want to thank Aitor Galarza, María del Mar del Arco, Vicente De Alba Mora, Javier Elorriaga, Edorta Unamuno, Jose Mari Unamuno and many volunteers. We further want to thank Tom Dries from

Thermal Focus for supplying thermal camera equipment and the Terrestrial Ecology Unit, Ghent University, for supplying additional wing samples. The wind tunnel was kindly provided by the Faculty of Bioscience Engineering, Ghent University. We thank Nele Delbecque for her assistance with the experimental set-up. We further deeply thank Annika Aurbach and Bram Vanthournout for their helpful comments on the manuscript and Sara Porchetta for her advice. We also thank the reviewers for their comments that helped improve this paper.

References

1. Hill GE, Hill GE, McGraw KJ. 2006 *Bird coloration: mechanisms and measurements*. Cambridge, MA: Harvard University Press.
2. Dale J, Dey CJ, Delhey K, Kempenaers B, Valcu M. 2015 The effects of life history and sexual selection on male and female plumage colouration. *Nature* **527**, 367–370. (doi:10.1038/nature15509)
3. Baker RR, Parker GA. 1979 The evolution of bird coloration. *Phil. Trans. R. Soc. Lond. B* **287**, 63–130. (doi:10.1098/rstb.1979.0053)
4. Walsberg GE. 1982 Coat color, solar heat gain, and conspicuousness in the Phainopepla. *Auk* **99**, 495–502.
5. Burtt Jr EH. 1981 The adaptiveness of animal colors. *BioScience* **31**, 723–729. (doi:10.2307/1308778)
6. Wolf BO, Walsberg GE. 2000 The role of the plumage in heat transfer processes of birds. *Am. Zool.* **40**, 575–584. (doi:10.1093/icb/40.4.575)
7. Walsberg GE, Campbell GS, King JR. 1978 Animal coat color and radiative heat gain: a re-evaluation. *J. Comp. Physiol. B Biochem. Syst. Environ. Physiol.* **126**, 211–222. (doi:10.1007/BF00688930).
8. Pennycuick CJ. 2008 *Modelling the flying bird*. Amsterdam, The Netherlands: Elsevier.
9. Pennycuick CJ. 1989 *Bird flight performance*. Oxford, UK: Oxford University Press.
10. Hassanalian M, Abdelmoula H, Ayed SB, Abdelkefi A. 2017 Thermal impact of migrating birds' wing color on their flight performance: possibility of new generation of biologically inspired drones. *J. Therm. Biol* **66**, 27–32. (doi:10.1016/j.jtherbio.2017.03.013)
11. Tobalske BW. 2007 Biomechanics of bird flight. *J. Exp. Biol.* **210**, 3135–3146. (doi:10.1242/jeb.000273)
12. Pennycuick C, Obrecht HH, Fuller MR. 1988 Empirical estimates of body drag of large waterfowl and raptors. *J. Exp. Biol.* **135**, 253–264.
13. Hassanalian M, Ayed S, Ali M, Houde P, Hocut C, Abdelkefi A. 2018 Insights on the thermal impacts of wing colorization of migrating birds on their skin friction drag and the choice of their flight route. *J. Therm. Biol* **72**, 81. (doi:10.1016/j.jtherbio.2018.01.011)
14. Hassanalian M, Throneberry G, Ali M, Ayed SB, Abdelkefi A. 2018 Role of wing color and seasonal changes in ambient temperature and solar irradiation on predicted flight efficiency of the albatross. *J. Therm. Biol* **71**, 112–122. (doi:10.1016/j.jtherbio.2017.11.002)
15. Bergman TL, Incropera FP, DeWitt DP, Lavine AS. 2011 *Fundamentals of heat and mass transfer*. Hoboken, NJ: John Wiley & Sons.
16. Ellington C. 2006 Insects versus birds: the great divide. In *Proc. 44th AIAA Aerospace Sciences Meeting and Exhibit, Reno, NV, 9–12 January 2006*, p. 35. Reston, VA: American Institute of Aeronautics and Astronautics.
17. Kjellén N, Hake M, Alerstam T. 2001 Timing and speed of migration in male, female and juvenile ospreys *Pandion haliaetus* between Sweden and Africa as revealed by field observations, radar and satellite tracking. *J. Avian Biol.* **32**, 57–67. (doi:10.1034/j.1600-048X.2001.320108.x)
18. Poole AF, Kirwan GM, Christie DA, Marks JS. Osprey (*Pandion haliaetus*). In *Handbook of the birds of the world alive* (eds J del Hoyo, A Elliott, J Sargatal, DA Christie, E de Juana). Barcelona, Spain: Lynx Edicions.
19. Levinson R. 2014 LBNL-SRI calculator. Lawrence Berkeley National Laboratory Heat Island Group. See https://www.usgbc.org/resources/lawrence-berkeley-national-laboratory-sri-calculator.
20. Bristow KL. 1987 On solving the surface energy balance equation for surface temperature. *Agric. For. Meteorol.* **39**, 49–54. (doi:10.1016/0168-1923(87)90015-3)
21. Handara VA, Illya G, Tippabhotla SK, Shivakumar R, Budiman AS. 2016 Center for Solar Photovoltaics (CPV) at Surya University: novel and innovative solar photovoltaics system designs for tropical and near-ocean regions (an overview and research directions). *Proc. Eng.* **139**, 22–31. (doi:10.1016/j.proeng.2015.09.211)
22. Tattersall GJ. 2016 Infrared thermography: a non-invasive window into thermal physiology. *Comp. Biochem. Physiol. A: Mol. Integr. Physiol.* **202**, 78–98. (doi:10.1016/j.cbpa.2016.02.022)
23. Al-Sanea SA, Zedan MF, Al-Ajlan SA, Abdul Hadi AS. 2003 Heat transfer characteristics and optimum insulation thickness for cavity walls. *J. Therm. Env. Build. Sci.* **26**, 285–307. (doi:10.1177/109719603027973).
24. Pennycuick CJ. 1997 Actual and 'optimum' flight speeds: field data reassessed. *J. Exp. Biol.* **200**, 2355–2361.
25. Shamoun-Baranes J, van Loon E. 2006 Energetic influence on gull flight strategy selection. *J. Exp. Biol.* **209**, 3489–3498. (doi:10.1242/jeb.02385)
26. Bruderer B, Boldt A. 2001 Flight characteristics of birds: I. Radar measurements of speeds. *Ibis* **143**, 178–204. (doi:10.1111/j.1474-919X.2001.tb04475.x)
27. Pennycuick CJ. 1987 Flight of auks (Alcidae) and other northern seabirds compared with southern Procellariiformes: ornithodolite observations. *J. Exp. Biol.* **128**, 335–347.
28. Osczevski RJ. 1995 The basis of wind chill. *Arctic* **48**, 372–382.
29. Dawson C, Vincent JF, Jeronimidis G, Rice G, Forshaw P. 1999 Heat transfer through penguin feathers. *J. Theor. Biol.* **199**, 291–295. (doi:10.1006/jtbi.1999.0959)
30. Lehmann B, Wakili KG, Frank T, Collado BV, Tanner C. 2013 Effects of individual climatic parameters on the infrared thermography of buildings. *Appl. Energy* **110**, 29–43. (doi:10.1016/j.apenergy.2013.03.066)
31. Faye E, Dangles O, Pincebourde S. 2016 Distance makes the difference in thermography for ecological studies. *J. Therm. Biol* **56**, 1–9. (doi:10.1016/j.jtherbio.2015.11.011)
32. Gabriels D, Cornelis W, Pollet I, Van Coillie T, Ouessar M. 1997 The ICE wind tunnel for wind and water erosion studies. *Soil Technol.* **10**, 1–8. (doi:10.1016/S0933-3630(96)00012-8)
33. Burnham K, Anderson D. 2002 *Model selection and multimodel inference*. New York, NY: Springer.
34. Minkina W, Dudzik S. 2009 *Infrared thermography: errors and uncertainties*. Chippenham, UK: John Wiley & Sons.
35. Lessells C, Boag PT. 1987 Unrepeatable repeatabilities: a common mistake. *Auk* **104**, 116–121. (doi:10.2307/4087240)
36. Team R. 2016 *RStudio: integrated development for R*. Boston, MA: RStudio, Inc.
37. Wickham H, Francois R, Henry L, Müller K. 2015 dplyr: a grammar of data manipulation. R Package v. 0.4. See https://dplyr.tidyverse.org.
38. Bates D, Maechler M, Bolker B, Walker S, Christensen RHB, Singmann H, Dai B, Grothendieck G. 2015 Package 'lme4'. *Convergence* **12**, 1–48. (doi:10.18637/jss.v067.i01)
39. Maia R, Eliason CM, Bitton PP, Doucet SM, Shawkey MD. 2013 pavo: an R package for the analysis, visualization and organization of spectral data. *Methods Ecol. Evol.* **4**, 906–913. (doi:10.1111/2041-210X.12069)
40. Wickham H. 2010 *Ggplot2: elegant graphics for data analysis (Use R!)*. New York: NY: Springer.
41. Bonser RH. 1995 Melanin and the abrasion resistance of feathers. *Condor-Kansas-* **97**, 590. (doi:10.2307/1369048)
42. Harper PW, Flanigan RE. 1950 The effect of rate of change of angle of attack on the maximum lift of a small model. NACA TN-2061. See https://ntrs.nasa.gov/archive/nasa/casi.ntrs.nasa.gov/19930082735.pdf.
43. Ward S, Rayner J, Möller U, Jackson D, Nachtigall W, Speakman J. 1999 Heat transfer from starlings *Sturnus vulgaris* during flight. *J. Exp. Biol.* **202**, 1589–1602.
44. Schmid SJ, Selberg BP. 1992 Analysis of the effect of heat strips on boundary layer development over a flat plate. SAE Technical Paper 921923. (doi:10.4271/921923)

45. Schmid S, Selberg B. 1993 Analysis of the effect of surface heating on boundary layer development over an NLS-0215 airfoil. In *11th Applied Aerodynamics Conference, Monterey, CA, 9–11 August 1993*, p. 3437. Reston, VA: American Institute of Aeronautics and Astronautics.
46. Pennycuick C. 2015 The flight of birds and other animals. *Aerospace* **2**, 505–523. (doi:10.3390/aerospace2030505)
47. Rogalla S, D'Alba L, Verdoodt A, Shawkey MD. 2019 Data from: Hot wings: thermal impacts of wing coloration on surface temperature during bird flight. Dryad Digital Repository. (doi:10.5061/dryad.hh23pt5)